Balancing of rotor-bearing systems without trial runs using the Numerical Assembly Technique - An experimental investigation

G. Quinz, M. Klanner, K. Ellermann
Graz University of Technology, Institute of Mechanics,
Kopernikusgasse 24/IV, 8010 Graz, Austria

Abstract
The balancing of flexible rotor-bearing systems is one of the most important challenges in the use of high-speed machinery. Since traditional balancing methods require multiple test runs, which are costly and time-consuming, the focus of modern balancing methods is to replace these with simulations. For this reason, two flexible rotor balancing methods based on the Numerical Assembly Technique (NAT) have been proposed by the present authors in recent years. The advantages of NAT are that it leads to quasi-analytical solutions and is very computationally efficient. In this paper, the methods are applied on a testbed consisting of an axial symmetric rotor running on anisotropic supports. The mode shapes, eigenvalues and unbalance responses are measured and compared to values calculated with NAT. The system is balanced and the reduction of vibration is determined. The results show that the procedure can be applied effectively.

1 Introduction

Unbalance is the main cause of rotor vibration, which reduces the life span of rotor-bearing systems and might be harmful to the surrounding. If the spin speed exceeds 70% of the first critical speed, the system is considered flexible and flexible balancing methods have to be used to reduce vibrations [1]. Traditional flexible balancing methods are gathered in two main groups: modal balancing methods and influence coefficient methods [2]. Both approaches can be significantly improved with a suitable rotor-dynamic model of the rotor-bearing system. For modal balancing methods [3], it is very advantageous to know the critical speeds and mode shapes of the system beforehand. This allows for the perfect placement of modal balancing weights, which minimizes the vibration of one mode without influencing any other mode. In the best-case scenario, if each critical speed can be surpassed safely before balancing and the rotor model is completely accurate, the system can be balanced with data from a single measurement run through all critical speeds [4]. Influence Coefficient methods [5] can be applied completely empirical and lead to good results as long as the rotor-bearings system is linear. However, the empirical approach requires a great number of test runs, which are expensive and time-consuming. On the other hand, if the influence coefficients are calculated with an accurate rotor-dynamic model these test runs can be avoided and only a measurement run to determine the initial unbalance of the rotor is necessary [6].
In this paper, the Numerical Assembly Technique (NAT) is applied to calculate eigenvalues, influence coefficients and mode shapes to allow the balancing of a rotor-bearing system.

NAT is an efficient, quasi-analytic method to calculate the steady-state harmonic response, modes and influence coefficients of rotor-bearing systems. In 1999, NAT was introduced by Wu and Chou as a method to compute the harmonic vibrations of one-dimensional structures [7, 8]. The method has been extended to additional applications in mechanics, especially in the field of rotor dynamics in subsequent years. Chen determined the natural frequencies of uniform beams using continuum models [9, 10, 11]. Lin analyzed the effects of multiple lumped masses, multiple-pinned supports, and rotary inertias on the calculation of Euler–Bernoulli beams [12, 13, 14]. In [15], these approaches were applied to the Timoshenko beam theory, and the effect of the slenderness ratio and the shear coefficient was investigated. Later Lin extended

both approaches [16, 17]. Yesilce examined the effects of axial forces on Timoshenko and Reddy-Bickford beams [18, 19, 20]. Later, Wu applied the method to rotating systems, determined the forward and backward whirling speeds and included gyroscopic effects [21]. Vaz analyzed the effect of various material and geometric discontinuities [22] and Farghaly examined Timoshenko beams on elastic supports [23]. In recent years, Klanner et al. introduced distributed loading [24], unbalance [25], and fractional derivative damping [26] in the NAT scheme. He also showed that NAT leads to a reduction of computational time by a factor of ten compared to FEM [25].

Recently, NAT has been applied to balance rotor-bearing systems with flexible behaviour. In [27], Quinz et al. proposed a method for the modal balancing of isotropic rotor-bearing systems using NAT. In the following year, another method was proposed, which is capable of balancing anisotropic rotor-bearing systems supported on fluid film bearings through calculated influence coefficients [28]. However, both methods were only applied to numerical simulations and there are no reports of systematic application of these balancing procedures in real-world test cases. The main aim of this work is to verify the feasibility of balancing methods based on NAT experimentally. For that, simulated unbalance responses are compared to measured data and a test case is balanced with the proposed method.

The remainder of this paper is organized as follows: Section 2 describes the simulation and balancing methods. Section 3 presents the test configuration and the obtained results. Section 4 discusses possible additions to the proposed method. Finally, Section 5 concludes the paper.

2 Methods

In this section, the applied simulation and balancing methods are described and the way in which those interact is explained.

2.1 Numerical Assembly Technique

The description of the Numerical Assembly Technique is adapted from the authors' previous work. For a more detailed description, the reader is referred to the papers by Klanner et. al. and Quinz et. al. [25, 26, 27, 28]. In Figure 1, the general rotor problem is shown.

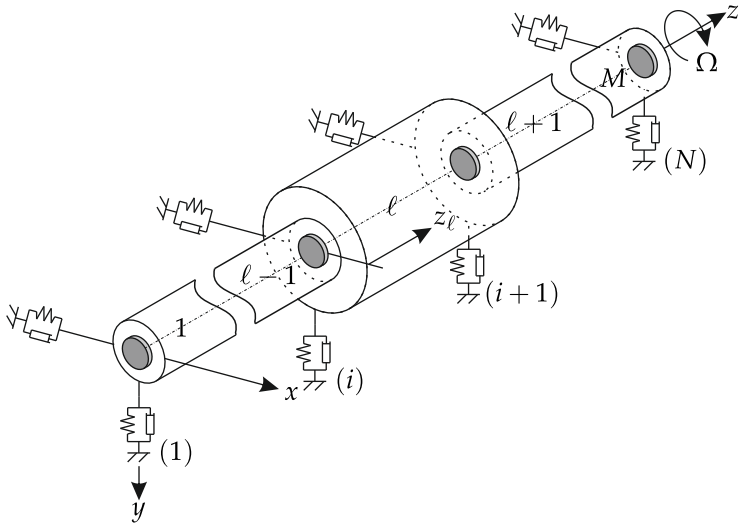

Figure 1: General rotor problem [28].

The space fixed coordinate system *Oxyz* is chosen so that *Oz* passes the undeflected axis of the rotor in its bearings. *Ox* and *Oy* are perpendicular to each other and transverse to *Oz*. For NAT, the rotor-bearing

system is divided into N stations and $M = N - 1$ segments. Stations represent disks, bearings, steps, and the ends of the rotor and are noted by the index in brackets and counted from $[(1), (2), ..., (i), ..., (N)]$. Segments represent the cylindrical elements between the stations and are counted from $[1, 2, ..., \ell, ..., M]$. The coordinate z_ℓ measures the distance in z-direction starting at the beginning of segment ℓ. The rotor is supported on an arbitrary amount of bearings modeled as anisotropic springs and dampers including cross-coupling terms and rotates at a constant spin speed Ω. The spring and damping coefficients may be spin speed dependent for example in the case of fluid film bearings. Several disks are mounted on the shaft. Each disk has a mass $m^{(i)}$, a mass moment of inertia about the x- and y-axis $\Theta_t^{(i)}$, a mass moment of inertia about the z-axis $\Theta_p^{(i)}$, an amount of eccentricity $\varepsilon^{(i)}$, and an angular position of eccentricity $\beta^{(i)}$. Segments are described by the Young's modulus E, density ρ_ℓ, area of the cross-section A_ℓ and its diametric moment of area of the cross-section about the x- and y-axis I_ℓ. The segments may also have a distributed unbalance defined by $\varepsilon_\ell(z)$ and $\beta_\ell(z)$ or be subject to external distributed forces $q_\bullet$. The rotor segments are modeled according to the Rayleigh beam theory, which has the same assumption as the Euler–Bernoulli beam theory, but includes rotary inertias and gyroscopic effects [29]. The state of the rotor is represented by the displacements u_x and u_y, the rotations of the cross-section φ_x and φ_y, the bending moments M_x and M_y and the shear forces Q_x and Q_y, which are all gathered in the solution vector $\vec{x}$. The equilibrium conditions lead to the equations of motion for any segment (index ℓ)

$$E_\ell I_\ell \frac{\partial^4 u_{x\ell}(z_\ell,t)}{\partial z_\ell^4} - \rho_\ell I_\ell \frac{\partial^4 u_{x\ell}(z_\ell,t)}{\partial z_\ell^2 \partial t^2} + \rho_\ell A_\ell \frac{\partial^2 u_{x\ell}(z_\ell,t)}{\partial t^2} - 2\rho_\ell I_\ell \Omega \frac{\partial^3 u_{y\ell}(z_\ell,t)}{\partial t \partial z_\ell^2} = q_x(z_\ell,t) + \rho_\ell A_\ell \varepsilon(z_\ell)\Omega^2 \cos(\Omega t + \beta(z_\ell)), \tag{1a}$$

$$E_\ell I_\ell \frac{\partial^4 u_{y\ell}(z_\ell,t)}{\partial z_\ell^4} - \rho_\ell I_\ell \frac{\partial^4 u_{y\ell}(z_\ell,t)}{\partial z_\ell^2 \partial t^2} + \rho_\ell A_\ell \frac{\partial^2 u_{y\ell}(z_\ell,t)}{\partial t^2} + 2\rho_\ell I_\ell \Omega \frac{\partial^3 u_{x\ell}(z_\ell,t)}{\partial t \partial z_\ell^2} = q_y(z_\ell,t) + \rho_\ell A_\ell \varepsilon(z_\ell)\Omega^2 \sin(\Omega t + \beta(z_\ell)). \tag{1b}$$

The rotations of the cross-section are defined by

$$\varphi_{y\ell}(z_\ell,t) = \frac{\partial u_{x\ell}(z_\ell,t)}{\partial z_\ell}, \tag{2a}$$

$$\varphi_{x\ell}(z_\ell,t) = -\frac{\partial u_{y\ell}(z_\ell,t)}{\partial z_\ell}, \tag{2b}$$

the bending moments are defined by

$$M_{y\ell}(z_\ell,t) = E_\ell I_\ell \frac{\partial^2 u_{x\ell}(z_\ell,t)}{\partial z_\ell^2}, \tag{3a}$$

$$M_{x\ell}(z_\ell,t) = -E_\ell I_\ell \frac{\partial^2 u_{y\ell}(z_\ell,t)}{\partial z_\ell^2}, \tag{3b}$$

and the shear forces can be computed by

$$Q_{x\ell}(z_\ell,t) = \rho_\ell I_\ell \frac{\partial^3 u_{x\ell}(z_\ell,t)}{\partial t^2 \partial z_\ell} + 2\rho_\ell I_\ell \Omega \frac{\partial^2 u_{y\ell}(z_\ell,t)}{\partial t \partial z_\ell} - E_\ell I_\ell \frac{\partial^3 u_{x\ell}(z_\ell,t)}{\partial z_\ell^3}, \tag{4a}$$

$$Q_{y\ell}(z_\ell,t) = \rho_\ell I_\ell \frac{\partial^3 u_{y\ell}(z_\ell,t)}{\partial t^2 \partial z_\ell} - 2\rho_\ell I_\ell \Omega \frac{\partial^2 u_{x\ell}(z_\ell,t)}{\partial t \partial z_\ell} - E_\ell I_\ell \frac{\partial^3 u_{y\ell}(z_\ell,t)}{\partial z_\ell^3}. \tag{4b}$$

Assuming a solution of the form

$$u_{x\ell}(z_\ell,t) = \tilde{u}_{x\ell}^{+}(z_\ell)\mathrm{e}^{\mathrm{i}\omega t} + \tilde{u}_{x\ell}^{-}(z_\ell)\mathrm{e}^{-\mathrm{i}\omega t}, \tag{5a}$$

$$u_{y\ell}(z_\ell,t) = \tilde{u}_{y\ell}^{+}(z_\ell)\mathrm{e}^{\mathrm{i}\omega t} + \tilde{u}_{y\ell}^{-}(z_\ell)\mathrm{e}^{-\mathrm{i}\omega t}, \tag{5b}$$

leads to four ordinary differential equations, where ω is the complex eigenvalue. The solutions of $u^{+}_{\bullet\ell}(z_\ell)$ and $u^{-}_{\bullet\ell}(z_\ell)$ have to be complex conjugated to yield a real solutions for $u_{\bullet\ell}(z_\ell, t)$. Therefore, the differential equations for $u^{+}_{\bullet\ell}(z_\ell)$ and $u^{-}_{\bullet\ell}(z_\ell)$ are completely decoupled, and only two of these equations

$$\begin{aligned}&\frac{\partial^4 \tilde{u}^{+}_{x\ell}(z_\ell)}{\partial z_\ell^4} + \rho_\ell \omega^2 \frac{\partial^2 \tilde{u}^{+}_{x\ell}(z_\ell)}{E_\ell \partial z_\ell^2}\\ &- \frac{\rho_\ell A_\ell \omega^2}{E_\ell I_\ell} \tilde{u}^{+}_{x\ell}(z_\ell) - 2\mathrm{i}\rho_\ell \Omega\omega \frac{\partial^2 \tilde{u}^{+}_{y\ell}(z_\ell)}{E_\ell \partial z_\ell^2} = \frac{\rho_\ell A_\ell \Omega^2}{2E_\ell I_\ell} \varepsilon(z_\ell) \mathrm{e}^{\mathrm{i}\beta(z_\ell)},\end{aligned} \tag{6a}$$

$$\begin{aligned}&\frac{\partial^4 \tilde{u}^{+}_{y\ell}(z_\ell)}{\partial z_\ell^4} + \rho_\ell \omega^2 \frac{\partial^2 \tilde{u}^{+}_{y\ell}(z)}{E_\ell \partial z_\ell^2}\\ &- \frac{\rho_\ell A_\ell \omega^2}{E_\ell I_\ell} \tilde{u}^{+}_{y\ell}(z_\ell) + 2\mathrm{i}\rho_\ell \Omega\omega \frac{\partial^2 \tilde{u}^{+}_{x\ell}(z_\ell)}{E_\ell \partial z_\ell^2} = -\frac{i\rho_\ell A_\ell \Omega^2}{2E_\ell I_\ell} \varepsilon(z_\ell) \mathrm{e}^{\mathrm{i}\beta(z_\ell)},\end{aligned} \tag{6b}$$

are sufficient to solve the system of equations. If steady-state vibrations due to unbalance are analyzed, it is apparent that $\Omega = \omega$. External distributed loadings $q_\bullet = 0$ can also be neglected in this case. The state within a rotor segment is defined by the matrix equation

$$\vec{x}_{h\ell}(z_\ell) = \underline{\underline{B}}_\ell(z_\ell)\vec{c}_\ell, \tag{7}$$

where $\vec{x}_{h\ell}$ is the homogeneous solution vector, $\underline{\underline{B}}_\ell$ is the state variable matrix, and $\vec{c}_\ell$ is a vector of arbitrary constants.

The total solution vector of a rotor segment consists of the homogeneous and the particular solution $\vec{x}_\ell(z_\ell) = \vec{x}_{h\ell}(z_\ell) + \vec{x}_{p\ell}(z_\ell)$. The particular solution depends on the unbalance, which can be considered either as point masses or as a distribution function. The state variable matrices of every station are assembled with the boundary and interface conditions into a system of linear equations

$$\underline{\underline{A}}\vec{c} = \vec{b}, \tag{8}$$

where $\underline{\underline{A}}$ is the system matrix, which depends only on the concentrated elements at the stations. The right-hand side vector $\vec{b}$ also depends on the unbalance. The unknown constants $\vec{c}$ are the solution of the system of linear equations, which defines the state variables of the whole rotor.

2.2 Modal balancing method

Modal balancing methods [30] allow progressively balancing a rotor-bearing system in the vicinity of critical speeds so that the modal components of unbalance are corrected without influencing already balanced modes. To achieve that, a modal matrix is needed, which consists of the relations of displacements of the rotor at each critical speed and each measure position. The modal matrix can either be measured, which is costly and time-consuming, approximated from previous measurements or calculated with an accurate rotor dynamic model. In the proposed method, the eigenvalues and the modal matrix are determined using NAT so that no trial runs are necessary and the system can be balanced with a single measurement run through all relevant critical speeds. In practice, it is often impossible to reach the information zones near the critical speeds with the unbalanced system so that an iterative approach is necessary [31].
For a detailed description of the way modal balancing methods work in conjuncture with NAT, the reader is referred to [27].

2.3 Influence coefficient method

Influence coefficient methods determine the ratio of displacements to unbalance forces and use this information to balance rotor-bearing systems. The advantage of these methods is that it is applicable to every

linear elastic rotor-bearing system and is not limited to lightly damped systems like modal balancing methods. Classical influence coefficient methods require many trial runs. This is avoided when the influence coefficients are calculated with an accurate rotor-dynamic model like NAT. Influence coefficients $\alpha_{ik}(\Omega)$ are defined as

$$\alpha_{ik}(\Omega) = \frac{x_i(\Omega)}{U_k}, \tag{9}$$

where $x_i(\Omega)$ is the displacement at position i caused by an unbalance U_k at position k. The influence coefficients of all combinations of unbalance planes k and measurement planes i are calculated and gathered in the influence coefficient matrix $\underline{\underline{\alpha}}$

$$\vec{x} = \underline{\underline{\alpha}}\vec{U}, \tag{10}$$

where $\vec{x}$ are the displacements of the rotor-bearing system caused by the addition of test weights and $\vec{U}$ is the unbalance vector. By inverting the influence coefficient matrix the initial unbalance is determined from the initial unbalance response

$$\vec{U}_c = -\underline{\underline{\alpha}}^{-1}\vec{x}_0, \tag{11}$$

where $\vec{U}_c$ are the correction unbalances, and $\vec{x}_0$ are the displacements of the rotor bearings system without test weights. The influence coefficient method can also include surplus information of additional measurement planes and spin speeds with the least-squares method [32].

3 Results

In this section, the setup and results of the practical test are described.

3.1 Testbed

In Figure 2, the rotor dynamic testbed of the Institute of Mechanic of the Graz University of Technology is shown. It consists of an elastic shaft with a maximal diameter of 15 mm, on which an arbitrary amount of disks can be mounted and which is supported on two roller bearings. The bearing housings are anisotropic with an anisotropy coefficient of 0.36986. The rotor-bearing system is excited by an electrical motor with a power of 7 kW and a maximum spin speed of 400 Hz. The unbalance response is measured with two triaxial acceleration sensors and four laser displacement measurement systems with an accuracy of 0.025 μm. The phase displacement is determined with an inductive sensor. The shaft is secured by a blast protection and two safety bearings, which allow for a maximal displacement of 1.5 mm.

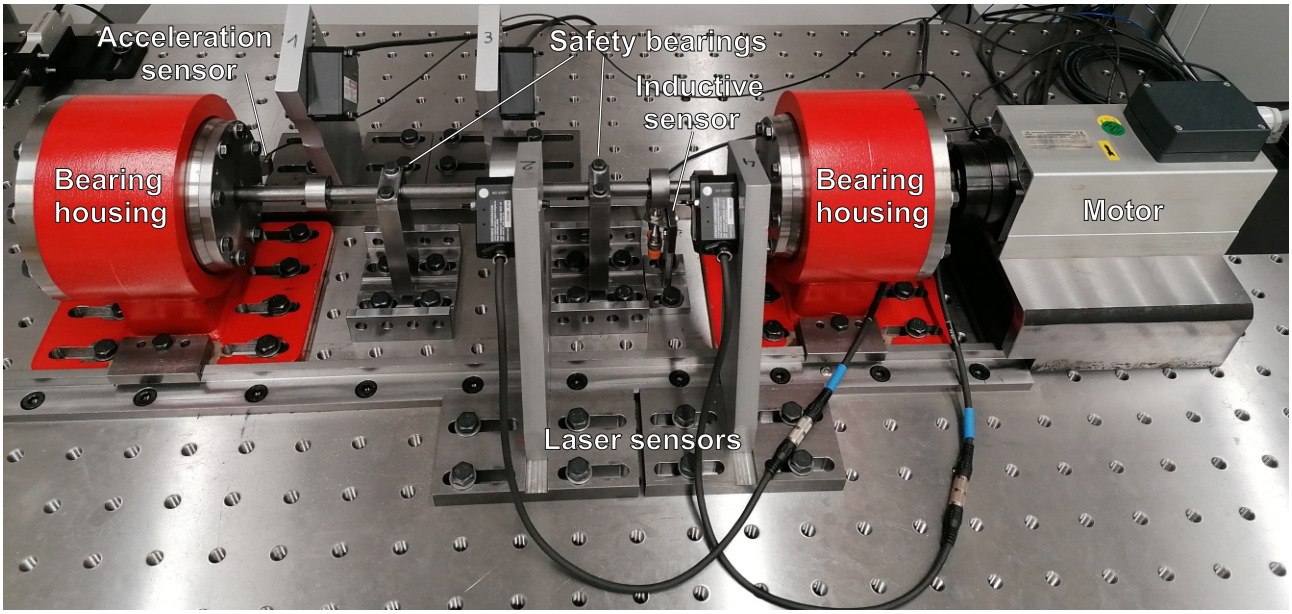

Figure 2: Rotor dynamic testbed (without blast protection.)

All calculations are performed on an *Intel*® Core™ i7-8700 CPU with 3.2 GHz running on a Windows 10 operating system using MATLAB™ version R2019a.

3.2 Modelling

For this paper, four disks of different weights are mounted on the rotor. The setup of the rotor-bearing system is shown in Figure 3.

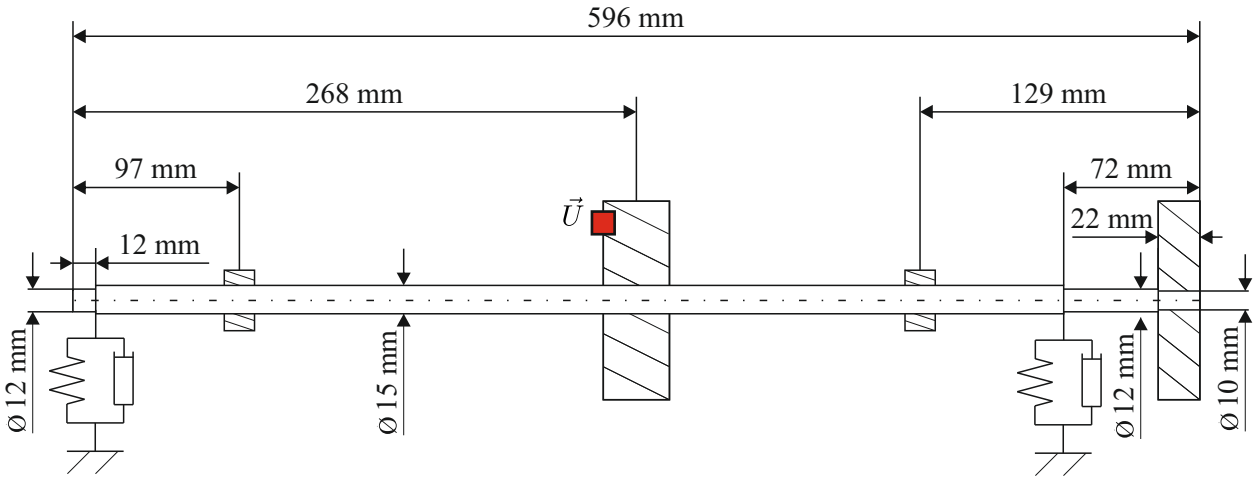

Figure 3: Configuration of the testbed

The system is modelled with NAT by the station parameters listed in Table 1. The segments are modelled with a Young's modulus of $2.19 \times 10^{11}\mathrm{N/m^2}$ and a density of 7700 $\mathrm{kg/m^3}$. The bearing parameters of this testbed were determined in [33].

Table 1: Stations of the NAT simulation

z	m	Θ_t	Θ_p	k_{xx}	k_{yy}	d_{xx}	d_{yy}
m	kg	kgm^2	kgm^2	N/m	N/m	Ns/m	Ns/m
0	0	0	0	0	0	0	0
0.008	0	0	0	2.8254×10^8	1.2997×10^8	80	80
0.097	0.1351	1.3418×10^{-5}	2.0398×10^{-5}	0	0	0	0
0.268	2.02	0.0015	0.0028	0	0	0	0
0.438	0.1351	1.3418×10^{-5}	2.0398×10^{-5}	0	0	0	0
0.574	0	0	0	2.8254×10^8	1.2997×10^8	80	80
0.585	0.6471	2.0322×10^{-4}	3.4134×10^{-4}	0	0	0	0
0.596	0	0	0	0	0	0	0

3.3 Balancing

The eigenvalues are determined by applying a recursive search algorithm on the system matrix of NAT. The first two eigenfrequencies are calculated within 0.60541 s and are 43.1089 Hz (backward whirling) and 43.3546 Hz (forward whirling). Detailed descriptions of the way eigenvalues are computed are found in [27] and [28]. Due to the bow of the shaft, the central disk has an unbalance equivalent to 297.5 g mm at the 60° position. The amplitude of displacement at the central disk at 35 Hz is measured to be 0.30698 mm. The result has to be corrected by the bow of the shaft and the unroundness of the disk, which have been determined at minimal spin speed to be 0.13 mm. Therefore, the excitation caused by unbalance is 0.17698 mm. For comparison, the displacement at the same position and spin speed with the known unbalance would be calculated with NAT to be 0.22211 mm. Using influence coefficients calculated with NAT, a balancing weight of 238.97 g mm at 240.4° is determined, within a computation time of 0.15432 s. Mounting this balancing weight causes a significant reduction of vibration shown in Figure 4. For the balanced system, a reduction of the vibration amplitude of 76.96% has been determined, which corresponds to a residual unbalance of 68.55 g mm. The measurement of the unbalanced vibration has been stopped at 42 Hz since an increase of the spin speed resulted in an amplitude above 1.5 mm and therefore rubbing at the safety bearings.

Table 2: Comparison of calculation to measurements

z	ω_{krit}	Amplitude	Correction unbalance	Balancing position
measured	45.5	0.17699 mm	297.5 g mm	240°
calculated	43.4	0.22211 mm	238.97 g	240.4°

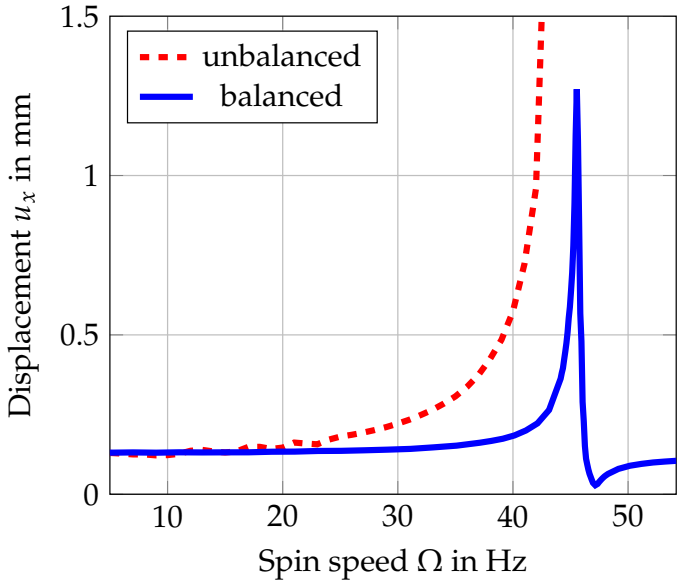

Figure 4: Balancing success

Although modal balancing is not necessary to balance a single mode, the mode shape of the first forward whirling mode is calculated with NAT and compared with measurements. As is seen in Figure 5 and Table 3, calculation and measurement are in good agreement.

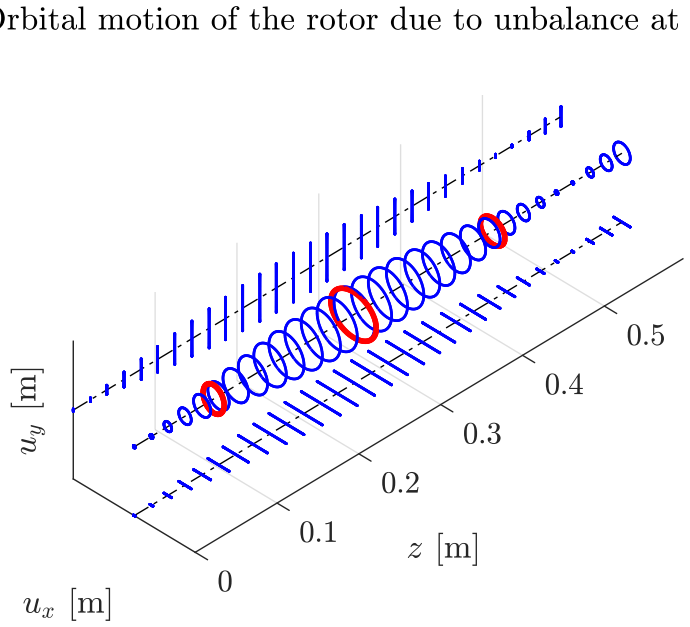

Figure 5: First mode shape: calculation in blue, measurement in red

Table 3: Dimensionless first mode shape

	$z = 0.097\mathrm{m}$		$z = 0.268\mathrm{m}$		$z = 0.438\mathrm{m}$	
	u_x	u_y	u_x	u_y	u_x	u_y
measured	0.4615	0.5462	0.8846	1	0.5380	0.50923
calculated	0.4622	0.4964	0.9315	1	0.4733	0.5085

Additional measurement data of this rotor configuration are found in [33].

4 Discussion

The proposed simulation method leads to a good approximation of the rotor behaviour and the system was successfully balanced. Differences between simulation and measurement are - besides inevitable measurement errors - caused by rotor dynamic phenomena which are not yet considered for this proof of concept. Effects already developed for NAT, which can easily be included are:

- Foundation influence: The proposed method can take multiple types of bearings like roller bearings or fluid film bearings into account. The effects of the bearing shield, bearing housing and foundation of the rotor-bearing system are neglected. Prem et al. [34] already developed a method to calculate modal masses and stiffness of the foundation by combining NAT with the Polynomial Chaos Kriging method. To unite this procedure with the proposed balancing approach might be useful for application with significant foundation influence.
- Shear forces: The Rayleigh beam theory is frequently used in rotor dynamic applications since it takes into account most rotor dynamic effects while still being numerically efficient. The Timoshenko beam theory also includes shear forces and is, therefore, more accurate at higher spin speeds. For this paper, the spin speeds of the experiments were low enough, that the differences between the beam theories are negligible.
- Internal damping: In many technical applications external damping far exceeds internal damping to avoid the destabilising effects of internal damping at supercritical speeds [35]. For systems without added external damping, the inclusion of the effects of internal damping may be useful. Methods to consider or determine fractional derivative damping parameters with NAT have been presented in [36, 37, 26].

An effect that is not yet included, but might be a useful addition to NAT, is:

- Residual bow: As measurements at low spin speeds show, the shaft of the test rotor is bent even without applied centrifugal forces. This effect influences the amplitude of vibration, depending on the angle between the direction of the bow and the unbalance response. Modal balancing of flexible rotors with bow using FEM has been performed by Deepthikumar et. al. [38].

Since the proof of concept was successful, the focus of further research is the extension of the proposed balancing technique and its application on more complex test cases.

5 Conclusion

In this paper, the feasibility of balancing flexible rotors using the Numerical Assembly Technique has been studied on a testbed. The method takes disks, a stepped shaft, anisotropic bearings and rotor dynamic effects like gyroscopy and rotary inertias into account. Simulation and measurement data for the eigenfrequencies, mode shapes and unbalance response are in good agreement. NAT is numerically efficient as the eigenvalues and the influence coefficients were computed in less than a second. The rotor-bearing system was successfully balanced with a reduction of vibration of 76.96%. After balancing, supercritical speeds were reached safely. The research indicates that the proposed balancing approach can be applied effectively.

Acknowledgements

The authors would like to thank Marcel S. Prem, Thiemo Klein and Michael Schoberleitner for their assistance in generating the measurement data.

References

[1] J. Tessarzik, R. Badgley, and W. J. Anderson, "Flexible rotor balancing by the exact point speed influence coefficient method," *J. Eng. Ind.*, vol. 94, pp. 145–158, 1972.

[2] L. Li, S. Cao, and J. Li, "Review of rotor balancing methods." *Machines*, vol. 9, p. 89, 2021.

[3] R. Bishop and G. Gladwell, "The vibration and balancing of an unbalanced flexible rotor." *Journal Mech. Eng. Soc.*, vol. 1, pp. 66–77, 1959.

[4] P. Gnielka, "Modal balancing of flexible rotors without test runs: An experimental investigation," *Journal of Vibrations*, vol. 90, no. 2, pp. 152–170, 1982.

[5] E. Thearle, "Dynamic balancing of rotating machinery in the field." *Trans. ASME*, vol. 56, pp. 745–753, 1934.

[6] R. Nordmann, E. Knopf, and B. Abrate, "Numerical analysis of the influence coefficient matrix for on-site balancing of flexible rotors." in *Proceedings of the 10th International Conference on Rotor Dynamics*, 2018, pp. 152–172.

[7] J.-S. Wu and H. M. Chou, "A new approach for determining the natural frequency of mode shapes of a uniform beam carrying any number of sprung masses," *Journal of Sound and Vibration*, vol. 220, no. 3, pp. 451–468, 1999.

[8] J.-S. Wu and D.-W. Chen, "Free vibration analysis of a Timoshenko beam carrying multiple spring masses by using the numerical assembly technique." *Int. J. Numer. Methods Eng.*, vol. 50, pp. 1039–1058, 2001.

[9] D.-W. Chen and J.-S. Wu, "The exact solutions for the natural frequencies and mode shapes of non-uniform multi-span beams with multiple spring mass systems." *J. Sound Vib.*, vol. 225, pp. 299–322, 2002.

[10] D.-W. Chen and J.-S. Wu, "The exact solutions for the natural frequencies and mode shapes of non-uniform multi-span beams carrying multiple various concentrated elements." *Structural Eng. Mech. Int. J.*, vol. 16, pp. 153–176, 2003.

[11] D.-W. Chen, "The exact solutions for free vibration of uniform beams carrying multiple two-degree-of-freedom spring-mass systems." *J. Sound Vib.*, vol. 295, pp. 342–361, 2006.

[12] H.-Y. Lin and Y.-C. Tsai, "On the natural frequencies and mode shapes of a uniform multi-step beam carrying multiple point masses," *Structural Eng. Mech. Int. J.*, vol. 21, pp. 351–367, 2005.

[13] H.-Y. Lin and Y.-C. Tsai, "On the natural frequencies and mode shapes of a multi-step beam carrying a number of intermediate lumped masses and rotary inertias." *Structural Eng. Mech. Int. J.*, vol. 22, pp. 701–717, 2006.

[14] H.-Y. Lin and Y.-C. Tsai, "Free vibration analysis of a uniform multi-span beam carrying multiple spring-mass systems." *Structural Eng. Mech. Int. J.*, vol. 302, pp. 442–456, 2007.

[15] J.-R. Wang, T.-L. Liu, and D.-W. Chen, "Free vibration analysis of a Timoshenko beam carrying multiple sping mass systems with the effect of shear deformation and rotary inertia." *Structural Eng. Mech. Int. J.*, vol. 26, pp. 1–14, 2007.

[16] H.-Y. Lin, "On the natural frequencies and mode shapes of a multi-span and multi-step beam carrying a number of concentrated elements." *Structural Eng. Mech. Int. J.*, vol. 29, pp. 531–550, 2008.

[17] H.-Y. Lin, "On the natural frequencies and mode shapes of a multi-span Timoshenko beam carrying a number of various concentrated elements." *J. Sound Vib.*, vol. 319, pp. 593–605, 2009.

[18] Y. Yesilce and O. Demirdag, "Effect of axial force on free vibration of timoshenko multi-span beam carrying multiple spring-mass systems." *Int. J. Mech. Sci.*, vol. 50, pp. 995–1003, 2008.

[19] Y. Yesilce, "Effect of axial force on the free vibration of a Reddy-Bickford multi-span beam carrying multiple spring-mass systems." *J. Vib. Control.*, vol. 16, pp. 11–32, 2010.

[20] Y. Yesilce, "Free vibrations of a Reddy-Bickford multi-span beam carrying multiple spring-mass systems." *Journal of Shock and Vibration*, vol. 18, pp. 709–726, 2011.

[21] J.-S. Wu, F.-T. Lin, and H.-J. Shaw, "Analytical solution for whirling speeds and mode shapes of a distributed-mass shaft with arbitrary rigid disks." *J. Appl. Mech.*, vol. 81, p. 034503, 2014.

[22] J. Vaz and J. de Lima junior, "Vibration analysis of Euler–Bernoulli beams in multiple steps and different shapes of cross section." *J. Vib. Control.*, vol. 22, pp. 193–204, 2016.

[23] S. Farghaly and T. El-Sayed, "Exact free vibration of a multi-step timoshenko beam system with several attachments." *Mech. Syst. Signal Process.*, vol. 72, pp. 525–546, 2016.

[24] M. Klanner and K. Ellermann, "Steady-state linear harmonic vibrations of multiple-stepped Euler-Bernoulli beams under arbitrarily distributed loads carrying any number of concentrated elements," *Applied and Computational Mechanics*, vol. 14, no. 1, pp. 31–50, 2019.

[25] M. Klanner, M. S. Prem, and K. Ellermann, "Steady-state harmonic vibrations of a linear rotor-bearing system with a discontinuous shaft and arbitrarily distributed mass unbalance," in *Proceedings of ISMA2020 International Conference on Noise and Vibration Engineering and USD2020 International Conference on Uncertainty in Structural Dynamics*, 2020, pp. 1257–1272.

[26] M. Klanner, M. Prem, and K. Ellermann, "Steady-state harmonic vibrations of viscoelastic Timoshenko beams with fractional derivative damping models." *Appl. Mech.*, vol. 2, pp. 789–819, 2021.

[27] G. Quinz, M. Prem, M. Klanner, and K. Ellermann, "Balancing of a linear elastic rotor-bearing system with arbitrarily distributed unbalance using the numerical assembly technique." *Bull. Pol. Acad. Sci. Tech. Sci*, vol. 69, p. e138237, 2021.

[28] G. Quinz, M. Prem, M. Klanner, and K. Ellermann, "Balancing of flexible rotors supported on fluid film bearings by means of influence coefficients calculated by the numerical assembly technique." *Energies*, vol. 15, no. 6, p. 2009, 2022.

[29] O. A. Bauchau and J. I. Craig, *Structural Analysis - With Applications to Aerospace Structures*. Heidelberg: Springer Verlag, 2009.

[30] R. E. D. Bishop and A. G. Parkinson, "On the isolation of modes in balancing of flexible shafts," *Proc. Inst. Mech. Eng.*, vol. 117, pp. 407–426, 1963.

[31] B. Xu and L. Qu, "A new practical modal method for rotor balancing." *Proc. Inst. Mech. Eng. Part C J. Mech. Eng. Sci.*, vol. 215, pp. 179–190, 2001.

[32] R. Nordmann, E. Knopf, and T. Krueger, "Balancing of flexible rotors by means of calculated influence coefficients." in *Proceedings of the SIRM 2021 International Conference on Dynamics of Rotating Machinery*, Gdansk, Poland, 2021, pp. 1–13.

[33] T. Klein, "Entwicklung eines Verfahrens zur Auslegung von Rotoren." Master's thesis, Graz University of Technology, Graz, Austria, 2021.

[34] M. S. Prem, M. Klanner, and K. Ellermann, "Model parameter estimation of ball bearings using generalized polynomial chaos expansion." in *Proceedings of SIRM 2021: The 14th International Conference on Dynamics of Rotating Machines*, 2021, pp. 331–340.

[35] G. Genta, *Dynamics of rotating systems*. Springer-Verlag, 2005.

[36] B. Blümel, M. Klanner, and K. Ellermann, "Investigation of steady-state harmonic axial and torsional vibrations of linear rotors under arbitrarily distributed loading using the numerical assembly technique," in *Proceedings of the 14th International Conference on dynamics of rotating machinery*, 2021, pp. 205–214.

[37] M. S. Prem, M. Klanner, and K. Ellermann, "Identification of fractional damping parameters in structural dynamics using polynomial chaos expansion." *Applied Mechanics*, vol. 2(4), pp. 956–975, 2021.

[38] M. B. Deepthikumar, A. S. Sekhar, and M. R. Srikanthan, "Modal balancing of flexible rotors with bow and distributed unbalance," *Journal of Sound and Vibration*, vol. 332, pp. 6216–6233, 2013.